

# Bacteriophobic Zwitterionic/Dopamine Coatings for Medical Elastomers

Robert Teixidó, Pol Cabanach, Richard Kaplan, Cristina García-Bonillo, Darío Pérez, Shuo Zhang, Salvador Borrós, and Abdon Pena-Francesch\*

Despite modern advancements in sterilization and medical practices, bacterial infections remain a significant concern in the implantation of medical devices. There is currently an urgent need for long-lasting and high-stable strategies to avoid the adhesion of bacteria to the wide range of materials present in medical devices. Here, a versatile methodology to create anti-biofouling coatings that prevent the adhesion of bacteria to silicone-based materials used in healthcare is reported. These coatings consist of bifunctional ethylene glycol dimethacrylate as an anchor between a zwitterionic polymer (SBMA), which provides antifouling properties, and a polydopamine layer that operates as an interfacial binder, providing mechanical strength and strong adhesion to elastomeric substrates. The coatings exhibit super-hydrophilic and anti-biofouling properties, creating a strong “bacteriophobic effect” that leads to a >99% reduction in bacterial adhesion. This bacteriophobic coating is successfully implemented and validated in a commercial urinary catheter, reducing bacterial adhesion by 1–2 orders of magnitude and avoiding bacterial colonization to prevent catheter-associated urinary tract infections. The results presented here demonstrate the versatility, durability, and scalability of the coating methodology for preventing bacterial adhesion in silicone elastomers, which can be easily applied to other elastomeric materials used in medical devices beyond urinary tract infection prevention.

bladder when they are unable to urinate on their own, relieving buildup of unwanted fluid collections, and administering medicines. During patient hospitalization, 17.5 to 23.6% of hospital patients undergo urinary catheterization, which typically leads to catheter-associated infections.<sup>[1]</sup> Catheter-associated urinary tract infections (CAUTIs) are commonly acquired in healthcare facilities, and arise from periurethral contamination and subsequent migration of uropathogenic bacteria through the urinary catheter to the bladder.<sup>[2–4]</sup> As a result, between 8.4 and 9.9 million of nosocomial CAUTIs occur in the United States annually, being the most common hospital-originated complication in the US,<sup>[5–7]</sup> representing an additional healthcare cost of \$451 million dollars/year.<sup>[8]</sup>

To fight against these types of infections and the formation of bacterial biofilms that cause them, a wide range of surface-engineering solutions have been developed for medical devices. Antimicrobial surfaces either make use of biocide release<sup>[9]</sup> or surface functionalities that kill


## 1. Introduction

Urinary catheters are one of the most ubiquitous medical devices in global healthcare. They are used to drain a patient's

bacteria on contact.<sup>[10]</sup> In contrast, antifouling surfaces prevent the initial adhesion of bacteria and the formation of biofilms through physical (surface topography modification) and/or chemical (surface chemistry modification) cues.<sup>[11]</sup> One of the most common antifouling strategy in medical devices consists in coating the device surface with hydrophilic polymers to hinder hydrophobic interactions to reduce the adhesion of proteins and bacteria.<sup>[12]</sup> For example, polyethylene glycol (PEG) and its derivatives are arguably the most widespread antifouling polymers in medical applications,<sup>[13,14]</sup> while zwitterionic polymers are emerging as a promising alternative<sup>[15,16]</sup> due to their enhanced antifouling and biofouling properties.<sup>[17–19]</sup> These polymers are typically grafted onto the surface of biomaterials to prevent protein and bacteria adhesion via hydration protective layers<sup>[20]</sup> and steric repulsion through mechanical agitation of their chains.<sup>[12,21]</sup> These antifouling coating methods have been extensively used in a wide array of applications and materials including micro/nanoparticles for drug delivery<sup>[22–24]</sup> and metal surfaces for biosensing.<sup>[25]</sup> Although they work reasonably well in rigid substrates (such as in gold electrodes),<sup>[26]</sup> these methods present severe limitations in flexible and stretchable materials

R. Teixidó, P. Cabanach, C. García-Bonillo, D. Pérez, S. Borrós  
Grup d'Enginyeria de Materials (GEMAT)  
Universitat Ramon Llull  
Via Augusta, 390, Barcelona 08017, Spain

R. Kaplan, S. Zhang, A. Pena-Francesch  
Materials Science and Engineering  
Macromolecular Science and Engineering  
University of Michigan  
2800 Plymouth Road, Ann Arbor, MI 48109, USA  
E-mail: abdon@umich.edu

 The ORCID identification number(s) for the author(s) of this article can be found under <https://doi.org/10.1002/admi.202201152>.

© 2022 The Authors. Advanced Materials Interfaces published by Wiley-VCH GmbH. This is an open access article under the terms of the Creative Commons Attribution License, which permits use, distribution and reproduction in any medium, provided the original work is properly cited.

DOI: 10.1002/admi.202201152

due to poor substrate adhesion, leading to delamination problems and decreased efficiency and durability. As a possible solution, polydopamine (pDA) coatings have been explored as a functional adhesion primer due to its catechol functionalities.<sup>[27]</sup> This pDA layer also contains free amines that can be modified through the aza-Michael reaction for further functionalization with other polymers. This method has been successfully used on multiple rigid materials such as titanium, TiO<sub>2</sub>, silicon, gold or polystyrene for antifouling functionalization.<sup>[28–30]</sup> However, this method often presents delamination, cracking, and uniformity problems when applied to soft and flexible substrates,<sup>[31]</sup> compromising their surface energy and antifouling properties.<sup>[28]</sup> Considering that urinary catheters (and most flexible medical devices) are fabricated from silicones that are hydrophobic, present high protein adhesion, and are difficult to modify chemically (due to the lack of reactive groups),<sup>[32,33]</sup> there is a need to develop effective and simple antifouling coating technologies that can be applied to soft, stretchable silicone substrates with complex geometries including but not limited to urinary catheters.

Here, we propose a facile fabrication scheme for the deposition of anti-biofouling polymer coatings with tunable properties on elastomeric silicone substrates using polydopamine, dimethacrylate linkers, and sulfobetaine. This method provides a robust anchoring of a zwitterionic film that is resistant to mechanical stress and preserves its superhydrophilic surface properties after several cycles of stretching, bending, and adhesion tests. We demonstrate a >99% reduction in bacterial adhesion on polydimethyl siloxane (PDMS) as our model medical-grade elastomeric silicone. We also validate our antibiofouling coating method in commercial urinary catheters, observing a reduction in bacteria colonization and observing a >99% reduction of bacterial adhesion against noncoated commercial catheters. The results presented here highlight the versatility and scalability of our method for preventing bacterial adhesion in silicone elastomers, which could be easily applied to other elastomeric materials used in medical devices beyond urinary tract infection prevention.

## 2. Results and Discussion

### 2.1. Multilayer Coating Strategy

Most flexible medical devices are made of silicone elastomers that are typically hydrophobic and chemically inert, which makes the functionalization challenging due to the lack of functional groups on the substrate surface. In addition to the chemical functionalization challenge, the coatings must resist the mechanical stresses associated to the normal operation of the flexible device, and therefore they must resist delamination and detachment while preserving its antibiofouling function. Furthermore, the coating method must be scalable and able to conformally coat complex geometries and hard-to-access areas in devices (such as the inner tubular cavities of urinary catheters). In order to achieve this, we have developed a solution-based multilayer coating strategy for the bacteriophobic functionalization of elastomeric substrates consisting on a polydopamine adhesive functional layer, a linker, and an antifouling polymer layer (Figure 1a).

We used PDMS as our model elastomer substrate to evaluate our method due to its biocompatibility, biostability, and its widespread use in medical applications as a medical-grade silicone. As the first step, polydopamine (pDA) was deposited on the elastomer substrate as an adhesive functional layer (Figure 1b). Despite the lack of functional groups in PDMS and other silicones, pDA was conformally deposited on silicones through their catechol groups.<sup>[34]</sup> pDA has amine groups that can be functionalized through the aza-Michael reaction,<sup>[35]</sup> and thus the initial pDA coating is used as a functional adhesive layer. This strategy has been previously used in the literature to attach functional polymers (including antibiofouling polymers) directly onto a pDA layer,<sup>[28]</sup> however, the coatings did not have enough stability and homogeneity to provide effective hydrophilicity and antibiofouling properties. To avoid this problem, we introduced a bifunctional linker to provide robust anchoring for subsequent layers. We used a dimethacrylated short linker (ethylene glycol dimethacrylate, EGDMA) as one methacrylate group can react with the dopamine amine (via

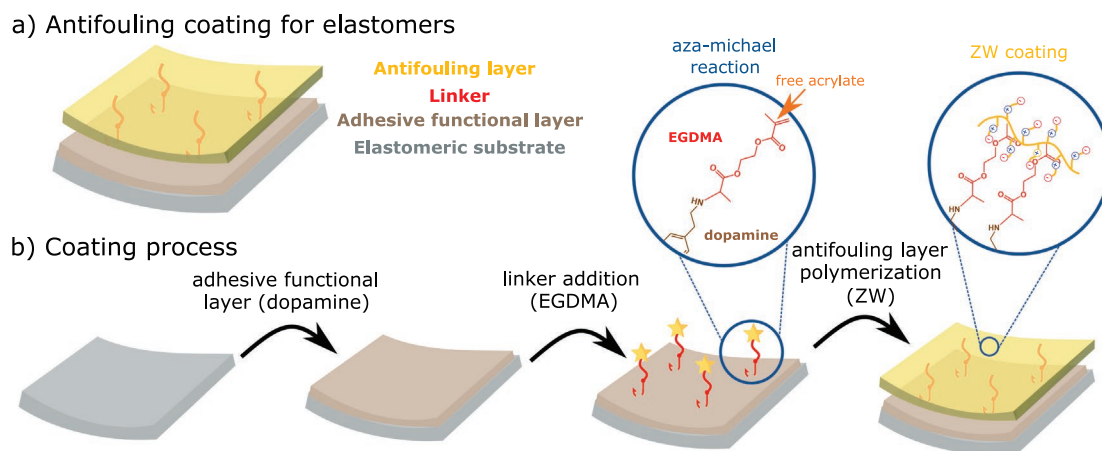


**Figure 1.** Zwitterionic anti-biofouling coating for elastomeric surfaces. a) Multilayer coating approach. b) A polydopamine layer bonds the zwitterionic layer to the elastomeric substrate using EGDMA as linker.

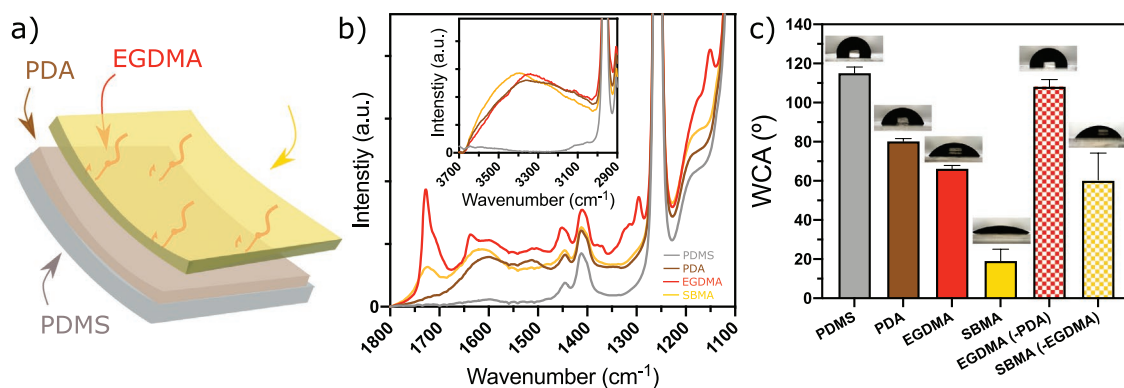


**Figure 2.** Structural and wetting analysis. a) Multilayer structure composed of (bottom to top) PDMS (substrate), PDA, EGDMA, and SBMA layers. b) FTIR spectra at each step of layer deposition. c) Water contact angle (WCA) at each step of layer deposition ( $n = 5$ , error bars are one standard deviation).

aza-Michael) while leaving the other methacrylate for further functionalization. In the last step, sulfobetaine methacrylate (SBMA) is polymerized with the free EGDMA methacrylate group via radical polymerization, forming a uniform zwitterionic final layer with high hydrophilicity and antibiofouling properties.

In order to validate the proposed coating method and verify the chemical composition after each step of the multilayer coating (Figure 2a), we performed Fourier transform infrared (FTIR) spectroscopy on PDMS coated samples. The FTIR spectra for each layer indicate a successful deposition after each coating step (Figure 2b). The deposition of polydopamine (pDA) onto a PDMS substrate is signified by bands at  $1600\text{ cm}^{-1}$  from its aromatic ring (C=C stretching) and  $3362\text{ cm}^{-1}$  from its primary amine (N-H stretching). Further addition of EGDMA via aza-Michael reaction is demonstrated by the emergence of a band at  $1740\text{ cm}^{-1}$  from its carbonyl group (C=O stretching). The deposition of a zwitterionic SBMA layer via free-radical polymerization is challenging to observe directly due to the fact that its most significant functional groups overlap with the bands of previous layers (notably dominated by the PDMS substrate). However, the successful SBMA deposition can be verified indirectly by measuring an increase in absorbed moisture in ambient conditions due to the increase hydrophilicity, observed as a shift in the amine-dominated band from  $3362$  to  $3393\text{ cm}^{-1}$  (O-H stretching).<sup>[36]</sup> The function of each layer can be further described by analyzing control samples with missing key steps in the process (Figure S1, Supporting Information). pDA provides an adhesion layer without which other molecules cannot adhere to PDMS substrates because of its lack of reactive groups (no EGDMA observed). Furthermore, the role of the EGDMA linker can be observed by the N-H/O-H shift due to a homogeneous zwitterionic layer anchored by EGDMA, which is not observed in the negative control samples without linker.

In order to further verify the successful coating and to analyze the wetting properties of each layer, water contact angle (WCA) measurements were performed on all samples (Figure 2c). Bare PDMS exhibited a large contact angle of  $115 \pm 3^\circ$ , which is expected due to its hydrophobic nature and agrees with previous reports.<sup>[37]</sup> With the deposition of the pDA layer, the WCA decreased to  $80.2 \pm 1.4^\circ$  due to the addition of a polar amine group to its surface. The EGDMA layer further

decreased the contact angle to  $66.2 \pm 1.7^\circ$  due to the incorporation of carbonyl groups from EGDMA, indicating the successful attachment of the linker molecule. When EGDMA was added to the PDMS substrate without a pDA adhesion layer, no significant differences were observed from the bare substrate, indicating that EGDA was not covalently attached. Last, when SBMA was added to pDA/EGDMA layer, WCA was reduced to superhydrophilic values ( $19 \pm 6^\circ$ ) indicating a successful zwitterionic surface modification. These low WCA values are characteristic of superhydrophilic zwitterionic surfaces, and agree with previous reports of zwitterionic coatings on rigid substrates.<sup>[28,38,39]</sup> However, previous coating methods on flexible substrates (consisting in direct functionalization of the pDA layer) did not provide a uniform zwitterionic coating resulting in higher contact angles ( $\approx 60^\circ$ ).<sup>[28]</sup> Our control experiments of direct functionalization of pDA with SBMA without EGDMA also presented higher contact values ( $60.5 \pm 13.7^\circ$ ), and demonstrated the need of a linker molecule to achieve good uniformity and stability of the zwitterionic film to preserve the superhydrophilic properties.

## 2.2. Mechanical Stability

The stability of the polymer coatings was tested to evaluate whether the surface properties were retained under mechanical stress. First, the adhesion of coated PDMS to a flat glass substrate was measured (Figure 3a) using previously established methods.<sup>[40]</sup> Briefly, a flat glass probe was loaded with a specified preload and contact time, and the maximum retraction force was measured and used to calculate the adhesion stress (Figure S2, Supporting Information). While PDMS substrates exhibited an adhesion of  $74 \pm 0.5\text{ kPa}$  (which agrees with previous reports<sup>[41,42]</sup>), each successive coating reduced the adhesion. This phenomenon can be clearly observed in the retraction force curves of each coating layer (Figure 3b, Supporting Information), where each successive coating step reduces the retraction force. The homogeneity of adhesion tests indicated that the coatings are not delaminated after several loading cycles, and thus can withstand repeated contact with other materials without compromising their structural integrity and surface properties. In addition to adhesion and

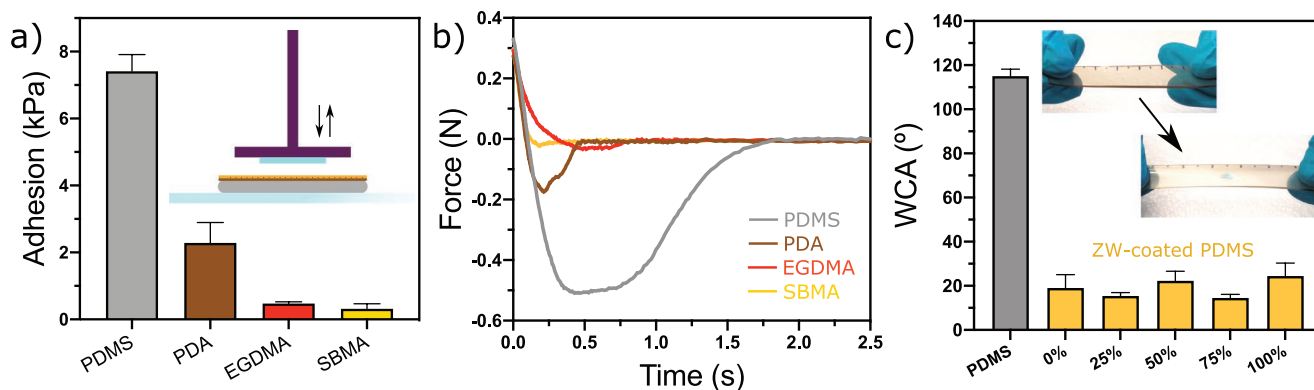


**Figure 3.** Mechanical stability of coated PDMS substrates. a) Adhesion after each deposited layer. b) Adhesion force curves for each deposited layer. c) WCA of ZW-coated PDMS under strain ( $n = 5$ , error bars are one standard deviation).

contact, the stability of the coatings was examined under substrate stretching (Figure 3c). The WCA of SBMA-coated PDMS substrates showed a decrease from  $115 \pm 3^\circ$  to  $19 \pm 6^\circ$  as previously discussed. Upon stretching to 25%, 50%, 75%, and 100% strain, the WCA did not significantly vary and remained within the range of unstretched samples. These results suggest that the coating was not damaged upon stretching and that the underlying substrate was not exposed, therefore preserving the surface properties. We also tested our coatings against other types of mechanical stress including torque (Figure S3, Supporting Information) and clamping (Figure S4, Supporting Information), which are relevant to the clinical application of these coatings to catheters. Good substrate adhesion is important to prevent coating delamination and loss of function in flexible devices, especially when subjected to clamping, torsion, and tension forces during implantation, handling, and overall operation. Hence, the coatings developed here can provide good durability and reliability as the mechanical stability and function are preserved under large mechanical stress and deformation.

### 2.3. Bacteriophobic Properties

After measuring the surface properties and mechanical stability of the zwitterionic coatings, we evaluated their bacteriophobic properties. First, we measured the adhesion of *Escherichia coli* CFT073 (a common uropathogenic clinical isolate) bacteria to bare PDMS control substrates (Figure 4a). Fluorescence imaging (with live/dead staining) after 24 h of incubation revealed a generalized presence of metabolically active bacteria and showed that the bacteria population adhered to PDMS was forming microcolonies, indicating the consolidation of the first stages of biofilm formation. This was observed both in bare PDMS and in fetal bovine serum (FBS)-treated PDMS, since adsorbed protein on the substrate surface can facilitate bacterial attachment.<sup>[43–45]</sup> SEM images of the incubated PDMS samples confirmed that bacteria were adhered forming an homogeneous monolayer. The presence of clusters distributed on the surface suggested the beginning of bacteria stratification, which indicates the irreversible formation of a biofilm. On the other hand, fluorescence images of zwitterionic-coated (ZW-coated) PDMS

substrates did not exhibit significantly large areas with live bacteria adhered to the surface (Figure 4b), in contrast with the uncoated PDMS controls. This fact demonstrates that the surface was able to prevent bacterial-surface interactions hindering the biofilm formation. The absence of dead bacteria (red) attached to the ZW surface is in good agreement with the fact that bacteria detachment is not caused by the release of potentially bactericidal agents present in the coating. Furthermore, FBS-treated ZW surfaces did not show an enhanced bacterial adhesion compared to nontreated surfaces, indicating that ZW surfaces hinder protein adsorption and avoid facilitating bacterial interactions and future adhesion processes.<sup>[22,46–48]</sup> In addition, SEM images of ZW-coated substrates showed only individual adhesion of bacteria to the surface without forming a structured monolayer and without forming a biofilm, validating the bacteriophobic coatings.

To further evaluate the coating performance in a bacterial rich environment for a long period of time, PDMS and ZW-coated samples were submerged on culture media with *E. coli* CFT073 for 50 h with a continuous refill of the bacterial growth medium to ensure bacterial viability (Figure 4c). After incubation, bacterial biofilm had grown to form a thick mucus structure. When removed from the media after incubation, coated and uncoated samples exhibited significant differences (Movie S1, Supporting Information). The biofilm was strongly adhered to the uncoated PDMS substrates, not detaching after removing the samples from the solution and aggressive washing. In contrast, bacteria were poorly adhered to the ZW-coated samples and were easily removed after gently rinsing the surface. This demonstrates that the zwitterionic coatings preserve their bacteriophobic properties and function after long incubation times and can prevent bacterial adhesion at different stages of biofilm growth, which is important for a performance assessment in realistic environments.<sup>[49]</sup> Last, the adhered bacteria on uncoated and ZW-coated PDMS samples was quantitatively analyzed (Figure 4d). The modification of PDMS substrates with ZW coatings reduced the number of adhered bacteria by 1–2 orders of magnitude (90–99%) in comparison with PDMS controls for the tested timeframe. The presence of FBS proteins enhanced the bacterial adhesion in both samples (uncoated and ZW-coated PDMS); however, ZW-coated samples did not reach the number of bacteria



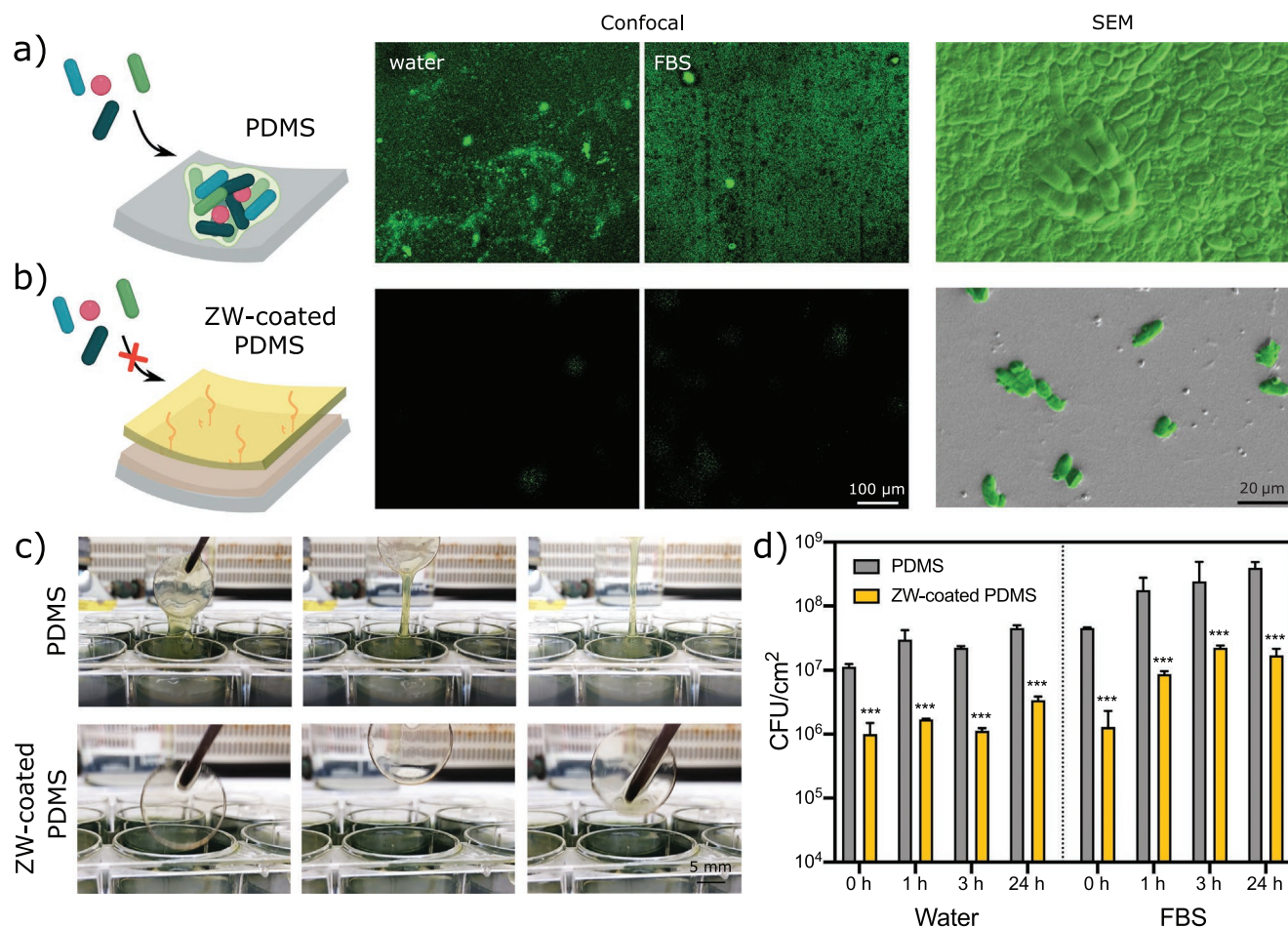


**Figure 4.** Bacterial adhesion to PDMS substrates. Surface characterization of a) uncoated PDMS and b) ZW-coated PDMS by confocal fluorescence and SEM, showing adhered bacteria in green. c) Growth of bacterial biofilm in uncoated (visible) and ZW-coated PDMS (not detected). d) Quantification of adhered bacteria on uncoated and ZW-coated PDMS ( $n = 3$ , error bars are one standard deviation, \*\*\* denotes  $P \leq 0.001$ ).

attached on PDMS in any case, remaining 2 orders of magnitude below uncoated PDMS controls.

#### 2.4. Validation in a Medical Device

Although the zwitterionic coatings on PDMS were effective and exhibited good hydrophilic and bacteriophobic properties as well as good adhesion to the substrate, they were performed on flat substrates. Working with real flexible devices such as a urinary catheter presents additional challenges that complicate the successful coating, including but not limited to complex geometries, inner cavities, homogeneity over large surfaces, etc. For this reason, we adapted our coating methodology to modify the inner walls of tubular structures and validated it in a commercially available urinary catheter. We verified the successful coating of the inner walls by FTIR (Figure 5a), with similar results than with flat surfaces (including the aromatic carbon stretching of pDA at  $1600\text{ cm}^{-1}$  and the carbonyl stretching of EGDMA and SBMA at  $1740\text{ cm}^{-1}$ ). WCA measurements (Figure 5b) on the inner walls of the catheter showed a drastic decrease of the contact angle with each coating step:  $103.1 \pm 2.7^\circ$  for the bare commercial catheter,  $79.3 \pm 0.8^\circ$  for

pDA,  $69.3 \pm 2.0^\circ$  for EGDMA, and  $32.8 \pm 6.1^\circ$  for SBMA. These results agree with those of flat substrates, and indicate that the coating of the inner catheter walls was successful. Furthermore, we evaluated the wetting properties of uncoated and ZW-coated catheters on an incline, and measured the spread of liquid (dye water) on the tubular structure (Figure 5c; Movie S2, Supporting Information). Commercial catheters were hydrophobic, which caused the droplets to slide fast but also to break up into smaller droplets that were pinned to the walls along the catheter. In a realistic medical scenario with urine, these small droplets can remain adhered to the surface and become sites of bacterial infection due to prolonged contact times. However, ZW-coated catheters were hydrophilic and exhibited a more homogeneous and continuous spread of the liquid that will facilitate its extraction.

To evaluate the bacteriophobic performance of our coatings in urinary catheters, ZW-coated and uncoated catheters were incubated with water or FBS for different times (0, 3, or 24 h). Then, *E. coli* CFT073 bacteria were incubated in the urinary catheters for more than 18 h ensuring biofilm formation inside the catheter lumen. Commercial urinary catheters without bacteria (above), commercial catheters with bacteria (middle) and ZW-coated catheters with bacteria (below) showed significant

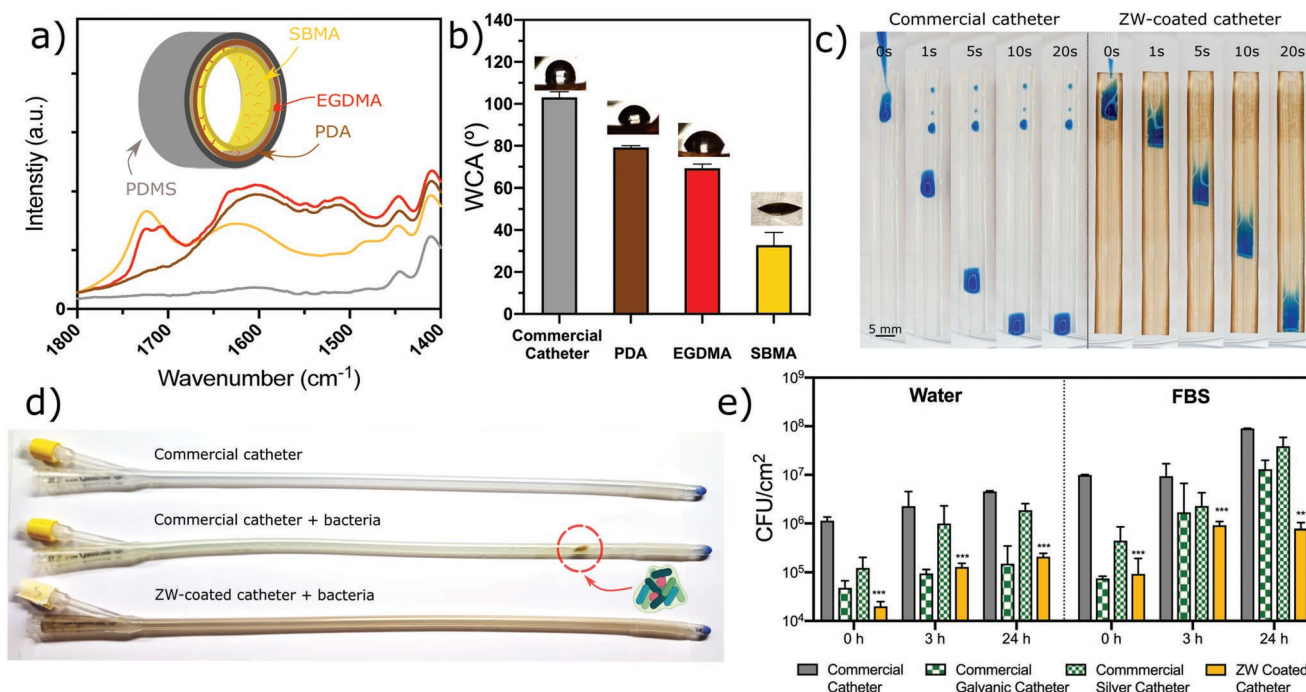


**Figure 5.** Anti-biofouling zwitterionic coatings in urinary catheters. a) FTIR spectra of coating layers inside a urinary catheter. b) WCA data of coating layers inside a urinary catheter. c) Wetting demonstration of surface-functionalized urinary catheters. d) Commercial and ZW-coated urinary catheters exposed to uropathogenic bacteria, exhibiting bacterial colonization in the uncoated catheter. e) Quantification of adhered bacteria on commercial, antibacterial, and ZW-coated catheters ( $n = 3$ , error bars are one standard deviation, \*\*\* denotes  $P \leq 0.001$ ).

differences in coloration after bacterial incubation (Figure 5d). After incubation, the commercial catheter showed a large biofilm mucus strongly attached to the lumen. After draining the entire catheter, biofilm remained adhered to the catheter inner surface (circled, in Figure 5d). It can be also observed how the catheter changed its transparent color to a greenish tone indicating strongly adhered bacteria to the catheter surface and the high production of pigment as virulence signals.<sup>[50,51]</sup> On the other hand, ZW-coated catheters avoided the formation of adhered biofilm and exhibited a homogeneous surface inside the tubular structure, preventing lumen blockage or narrowing the inner diameter by the biofilm. ZW-coated catheters showed a brownish coloration, however, this is caused by the polydopamine coating and not by the bacteria.<sup>[34]</sup> Furthermore, bacterial counts were evaluated on urinary catheter samples after bacterial incubation for a quantitative analysis of the bacteriophobic properties of the coated catheter (Figure 5e). Similar results to those observed on PDMS flat coupons were obtained, validating the reproducibility of the coating on real medical devices. ZW-coated catheters have shown a reduction in bacterial adhesion throughout the entire drainage tube. In ZW-coated catheters, bacterial adhesion was reduced by 1–2 orders of magnitude in all cases, including urinary catheters previously incubated with FBS. In contrast, commercial urinary catheters significantly increased the adhered bacteria to lumen after being in contact with FBS. This fact demonstrates that the zwitterionic surface on ZW-coated catheters also reduces the enhanced bacterial growth caused by adsorbed protein, thus hindering bacterial adhesion and biofilm formation on commercial urinary catheter.

In addition to uncoated commercial catheters, commercial urinary catheters with two different antimicrobial strategies have also been evaluated for comparison: an antimicrobial commercial catheter based on silver release (release of silver ions from a hydrogel coating on the lumen) and an antimicrobial commercial catheter based on galvanic effect (caused by the selective immobilization of different metals on the inner surface of the device). The silver release catheter exhibited adhered bacteria concentrations similar to the base commercial catheter in water ( $\approx 10^6$  CFU  $\text{cm}^{-2}$ ) and in FBS ( $\approx 10^8$  CFU  $\text{cm}^{-2}$ ) only in the first 3 h of incubation, indicating that this method loses effectivity after 3 h (probably due to the diffusion of silver ions to the media at concentrations below the minimum inhibitory concentration). The galvanic antimicrobial catheter shows a reduction on bacteria adhesion similar to the ZW-coated catheter when incubated in water. However, when incubated in FBS (protein-rich medium that promotes bacterial adhesion), the galvanic catheter reaches similar levels of bacteria as adhered to the other controls. Under the evaluated conditions, the bacteria adhesion reduction provided by the ZW coating outperforms the three commercial urinary catheters (including two antimicrobial commercial catheters) by 1–2 orders of magnitude.

### 3. Conclusion

We have designed and characterized a functionalization methodology for the obtention of a high-stable antifouling coating that reduces significantly (by 1–2 orders of magnitude) the adhesion of bacteria to elastomeric substrates, hence avoiding

the formation of biofilm structures. The coating was developed by a simple and direct immobilization of poly-sulfobetaine macromolecules on a polydopamine substrate through a dimethacrylate linker using aza-Michael reaction. This scalable methodology provides a good substrate adhesion preventing coating delamination and preserving superhydrophobic and anti-biofouling surface properties. These properties play a critical role avoiding bacterial adhesion on a wide range of substrates, reaching a reduction of >99% validated through bacterial quantification, microscopy of immobilized bacteria, and macroscopic observation of the formed mucus biofilm. This approach also offers several other advantages for its clinical application, including the ability to be implemented in complex shapes and sizes by an easy modification process, as we demonstrate by functionalizing a commercial medical device such as the urinary catheter. The characterization of coated urinary catheters under CAUTI-relevant environments revealed that our coating maintains the bacteriophobic properties and the mechanical performance, as well as avoids bacteria adhesion and biofilm formation inside the urinary catheter. The effectiveness of the coating in reducing bacterial adhesion outperforms that of two commercial antibacterial strategies, especially in bioenvironments with high protein content. This coating methodology provides a solution for the control of CAUTIs in urinary catheters, but due to its versatility and scalability, it can also be applied to other device-relevant substrates and materials including flexible biocompatible elastomers to prevent bacterial colonization and biofilm development in a variety of medical devices.

#### 4. Experimental Section

**Deposition of Polydopamine (PDA) Interfacial Binder Layer:** A Tris buffer solution was prepared at a concentration of 6 g L<sup>-1</sup> and titrated to a pH of 8.5 using 0.1 M HCl solution. A 1.4 mg mL<sup>-1</sup> solution of dopamine hydrochloride in Tris buffer was prepared and poured into a reaction container. PDMS substrates were placed on the surface of the solution, and polymerization on the submerged side of the PDMS was allowed to occur overnight. Coated samples were then rinsed with DI water to remove excess dopamine and stored.

**Deposition of EGDMA Linker Layer:** A Bicine buffer solution was prepared at a concentration of 8.15 g L<sup>-1</sup> and titrated to a pH of 8.8 using 0.1 M NaOH solution. A 11.25 μL mL<sup>-1</sup> solution of ethylene glycol dimethacrylate (EGDMA) in Bicine buffer was prepared and poured into a reaction container. PDA-coated PDMS substrates were placed on the surface of the solution overnight and rinsed with DI water to remove excess EGDMA.

**Deposition of SBMA Antifouling Layer:** PDMS samples (after pDA and REGDMA coating) were placed in a solution of 10 mg mL<sup>-1</sup> 4,4'-azobis(4-cyanovaleric acid) (V-501) and 0.2 M of sulfobetaine methacrylate (SBMA). The reaction assembly was placed in an oven at 70 °C and allowed to polymerize overnight and rinsed with DI water to remove excess reagents.

**Infrared Spectroscopy:** Coated elastomeric substrates were analyzed by Fourier transform infrared spectroscopy (FTIR) in a ThermoFisher Nicolet iS20 with a platinum ATR accessory, using 128 scans at 4 cm<sup>-1</sup> resolution.

**Water Contact Angle:** 10 μL DI water droplets were placed on the functionalized substrates and devices, and images were taken with a Dino-Lite AM73915MZTL (R10A) digital microscope with an imaging software (Dinocapture 2.0). Contact angle images were analyzed in ImageJ.

**Mechanical Stability Tests:** The experiments were performed in a Discovery HR 30 rheometer (TA Instruments) with custom parallel plates to measure the adhesion between the coated substrates and flat borosilicate glass substrates. Samples were loaded at a constant linear rate of 5 μm s<sup>-1</sup> to a constant compression preload force which was maintained for 30 s. Samples were unloaded at a constant linear rate of 20 μm s<sup>-1</sup> until the two substrates detach. This cycle was repeated multiple times to detect coating delamination or detachment.

**Bacterial Culture:** Bacterial strain was purchased from ATCC, The Global Bioresource Centre in United States of America. The strain used was *Escherichia coli* CFT073 (ATCC 700928), which is a gram-negative uropathogenic bacteria (human clinical isolate) strain. A single colony from the stock of each strain was cultured in 50 mL of appropriated growth media (Luria Bertani (LB) at 37 °C with overnight agitation to obtain the initial inoculum. Bacteria growth was observed through optical density at 600 nm in a spectrophotometer (Spectramax M2, Molecular Devices, USA) between 18 to 50 h at 37 °C.

**Bacterial Adhesion Tests:** Bacterial inoculum was diluted in fresh media and grown to OD 0.02 (600 nm). The bacteria were incubated with sample coupons placed on 24-well cell culture plate in static conditions at 37 °C overnight (≈18 h). After bacterial incubation, samples were removed from wells and washed twice in sterile PBS at room temperature to remove nonattached bacteria. Samples were then placed in sterile tubes with 2 mL of PBS and the tubes were sonicated for 10 min at 70 Hz, vortex for 2 min and sonicated again for 10 min. Bacterial pellets were collected at 4500 × g for 20 min, rinsed twice and resuspended in sterile PBS, to perform serial dilutions. Serial dilutions were made in PBS. Bacteria were plated in tryptic soy-agar (TSA) plates and incubated at 37 °C between 18 to 36 h to count total colony forming units (CFUs).

**Bacterial Visualization FE-SEM:** To test bacterial adhesion on surfaces by FE-SEM, initial inoculum of *E. coli* CFT073 was diluted in fresh media and grown to OD 0.02 (600 nm) and the bacteria were then put in contact with coupons in static conditions at 37 °C overnight. Surfaces were washed twice in sterile PBS at room temperature to remove nonattached bacteria. The attached bacteria on samples were then fixed adding 4% formaldehyde at room temperature for at least 2 h. To keep the size of bacteria, formaldehyde was washed with sterile PBS and a serial dehydration using ethanol 30%, 50%, 70% (30 min each) with a final wash in ethanol 90%. After that, a gold sputtered coating was performed on the samples to enhance electron conductivity. The images were artificially colored in green to improve the visualization of the bacteria.

**Bacterial Visualization Fluorescence Microscopy:** Surfaces incubated with *E. coli* CFT073 were prepared according to the protocol provided by the manufacturer with the kit LIVE/DEAD BacLight Bacterial Viability kit, L7007 (ThermoFisher, USA) to obtain confocal microscopy images to visualize live (green fluorophore, SYTO 9) or dead (red fluorophore, Propidium iodide) bacteria. Images were obtained using a Scanning Confocal Microscopy Leica SP-8.

**Coating of Catheters:** The coating of the catheters was done following the same steps used for the PDMS substrates. The catheters were filled with the different solutions and a cap was used to prevent any leakage.

**Statistical Analysis:** Data is presented as mean ± standard deviation throughout the manuscript. Sample size for each statistical analysis is  $n = 5$  for WCA and mechanical tests, and  $n = 3$  for bacterial adhesion tests. GraphPad and Origin software were used to analyze the data and present the figures. TRIOS software (TA Instruments), OMNIC (ThermoFisher), Dinocapture (Dino-Lite), and ImageJ were used for data collection and analysis for mechanical adhesion, FTIR, and WCA respectively.

#### Supporting Information

Supporting Information is available from the Wiley Online Library or from the author.



## Acknowledgements

The authors thank the Generalitat de Catalunya for the Research Consolidated Group Grant (2017 SGR 1559) to Grup d'Enginyeria de Materials (GEMAT) and the University of Michigan College of Engineering for startup funds.

## Conflict of Interest

The authors declare no conflict of interest.

## Authors Contribution

R.T. and P.C. contributed equally to this work. S.B., R.T., and A.P.F. conceived the idea; S.B., R.T., and A.P.F. proposed and designed the research; R.T. and A.P.F. designed the experiments; P.C., R.K., C.G.B., D.P., and S.Z. performed the experiments under the supervision of R.T. and A.P.F. The methodology was validated by A.P.F., P.C., and R.K. The results were analyzed by R.T., A.P.F., P.C., R.K., and C.G.B.; R.K., P.C., R.T., and A.P.F. wrote the manuscript. All authors have contributed to the editing of the manuscript and have read and agreed to the published version of it.

## Data Availability Statement

The data that support the findings of this study are available from the corresponding author upon reasonable request.

## Keywords

antibiofouling, bacteriophobic coatings, biopolymer, medical device, medical elastomer, urinary catheter, zwitterionic polymer

Received: May 24, 2022

Revised: July 30, 2022

Published online: September 9, 2022

- [1] L. E. Nicolle, *Antimicrob. Resist. Infect. Control* **2014**, *3*, 1.
- [2] A. S. Leticia-Kriegel, H. Salmasian, D. K. Vawdrey, B. E. Youngerman, R. A. Green, E. Y. Furuya, D. P. Calfee, R. Perotte, *BMJ Open* **2019**, *9*, e022137.
- [3] N. Sabir, A. Ikram, G. Zaman, L. Satti, A. Gardezi, A. Ahmed, P. Ahmed, *Am. J. Infect. Control* **2017**, *45*, 1101.
- [4] A. L. Flores-Mireles, J. N. Walker, M. Caparon, S. J. Hultgren, *Nat. Rev. Microbiol.* **2015**, *13*, 269.
- [5] D. K. Newman, J. wound, ostomy, C. , *Nurs. Off. Publ. Wound, Ostomy Cont. Nurses Soc.* **2007**, *34*, 655.
- [6] B. W. Trautner, R. O. Darouiche, *Arch. Intern. Med.* **2004**, *164*, 842.
- [7] L. E. Nicolle, *Drugs Aging* **2005**, *22*, 627.
- [8] Z. Zhu, Z. Wang, S. Li, X. Yuan, *J. Biomed. Mater. Res., Part A* **2019**, *107*, 445.
- [9] E. M. Hetrick, M. H. Schoenfisch, *Chem. Soc. Rev.* **2006**, *35*, 780.
- [10] E. R. Kenawy, S. D. Worley, R. Broughton, *Biomacromolecules* **2007**, *8*, 1359.
- [11] A. Dhyani, J. Wang, A. K. Halvey, B. Macdonald, G. Mehta, A. Tuteja, *Science* **2021**, *373*, 321.
- [12] S. Chen, L. Li, C. Zhao, J. Zheng, *Polymer* **2010**, *51*, 5283.
- [13] J. M. Harris, R. B. Chess, *Nat. Rev. Drug Discovery* **2003**, *2*, 214.
- [14] F. M. Veronese, A. Mero, *BioDrugs* **2008**, *22*, 315.
- [15] L. Zheng, H. S. Sundaram, Z. Wei, C. Li, Z. Yuan, *React. Funct. Polym.* **2017**, *118*, 51.
- [16] J. B. Schlenoff, *Langmuir* **2014**, *30*, 9625.
- [17] J. Ladd, Z. Zhang, S. Chen, J. C. Hower, S. Jiang, *Biomacromolecules* **2008**, *9*, 1357.
- [18] Z. Cao, L. Zhang, S. Jiang, *Langmuir* **2012**, *28*, 11625.
- [19] H. Vaisocherová, W. Yang, Z. Zhang, Z. Cao, G. Cheng, M. Piliarik, J. Homola, S. Jiang, *Anal. Chem.* **2008**, *80*, 7894.
- [20] S. Jiang, Z. Cao, *Adv. Mater.* **2010**, *22*, 920.
- [21] B. Dong, S. Manolache, A. C. L. Wong, F. S. Denes, *Polym. Bull.* **2011**, *66*, 517.
- [22] P. Cabanach, A. Pena-Francesch, D. Sheehan, U. Bozuyuk, O. Yasa, S. Borros, M. Sitti, *Adv. Mater.* **2020**, *32*, 2003013.
- [23] A. Biosca, P. Cabanach, M. Abdulkarim, M. Gumbleton, C. Gómez-Canela, M. Ramírez, I. Bouzón-Arnáiz, Y. Avalos-Padilla, S. Borros, X. Fernández-Busquets, *J. Controlled Release* **2021**, *331*, 364.
- [24] X. Han, Y. Lu, J. Xie, E. Zhang, H. Zhu, H. Du, K. Wang, B. Song, C. Yang, Y. Shi, Z. Q. Cao, *Nat. Nanotechnol.* **2020**, *15*, 605.
- [25] J. Baggerman, M. M. J. Smulders, H. Zuilhof, *Langmuir* **2019**, *35*, 1072.
- [26] Y.-S. Wang, S. Yau, L.-K. Chau, A. Mohamed, C.-J. Huang, *Langmuir* **2019**, *35*, 1652.
- [27] A. R. Statz, R. J. Meagher, A. E. Barron, P. B. Messersmith, *J. Am. Chem. Soc.* **2005**, *127*, 7972.
- [28] C. Y. Liu, C. J. Huang, *Langmuir* **2016**, *32*, 5019.
- [29] L. Q. Xu, D. Pranantyo, K. G. Neoh, E. T. Kang, S. L. M. Teo, G. D. Fu, *Polym. Chem.* **2016**, *7*, 493.
- [30] A. Golabchi, B. Wu, B. Cao, C. J. Bettinger, X. T. Cui, *Biomaterials* **2019**, *225*, 119519.
- [31] W. Zhang, F. K. Yang, Y. Han, R. Gaikwad, Z. Leonenko, B. Zhao, *Biomacromolecules* **2013**, *14*, 394.
- [32] H. Zhang, M. Chiao, *J. Med. Biol. Eng.* **2015**, *35*, 143.
- [33] Y. Yu, H. Yuk, G. A. Parada, Y. Wu, X. Liu, C. S. Nabzdyk, K. Youcef-Toumi, J. Zang, X. Zhao, *Adv. Mater.* **2019**, *31*, 1807101.
- [34] H. Lee, S. M. Dellatore, W. M. Miller, P. B. Messersmith, *Science* **2007**, *318*, 426.
- [35] A. B. Asha, Y. Chen, R. Narain, *Chem. Soc. Rev.* **2021**, *50*, 11668.
- [36] H. Kitano, T. Mori, Y. Takeuchi, S. Tada, M. Gemmei-Ide, Y. Yokoyama, M. Tanaka, *Macromol. Biosci.* **2005**, *5*, 314.
- [37] T. Trantidou, Y. Elani, E. Parsons, O. Ces, *Microsyst. Nanoeng.* **2017**, *3*, 16091.
- [38] Y.-F. Yang, Y. Li, Q.-L. Li, L.-S. Wan, Z.-K. Xu, *J. Memb. Sci.* **2010**, *362*, 255.
- [39] M. Kobayashi, Y. Terayama, H. Yamaguchi, M. Terada, D. Murakami, K. Ishihara, A. Takahara, *Langmuir* **2012**, *28*, 7212.
- [40] V. Sariola, A. Pena-Francesch, H. Jung, M. Çetinkaya, C. Pacheco, M. Sitti, M. C. Demirel, *Sci. Rep.* **2015**, *5*, 13482.
- [41] D. M. Drotlef, C. B. Dayan, M. Sitti, *Integr. Comp. Biol.* **2019**, *59*, 227.
- [42] M. Zhou, Y. Tian, D. Sameoto, X. Zhang, Y. Meng, S. Wen, *ACS Appl. Mater. Interfaces* **2013**, *5*, 10137.
- [43] R. Orme, C. W. I. Douglas, S. Rimmer, M. Webb, *Proteomics* **2006**, *6*, 4269.
- [44] P. J. Molino, M. J. Higgins, P. C. Innis, R. M. I. Kapsa, G. G. Wallace, *Langmuir* **2012**, *28*, 8433.
- [45] C. García-Bonillo, R. Teixidó, G. Reyes-Carmenaty, J. Gilabert-Porres, S. Borrós, *ACS Appl. Biol. Mater.* **2020**, *3*, 3354.
- [46] L. Mi, S. Jiang, *Angew. Chem., Int. Ed.* **2014**, *53*, 1746.
- [47] L. Zhang, Z. Cao, T. Bai, L. Carr, J.-R. Ella-Menye, C. Irvin, B. D. Ratner, S. Jiang, *Nat. Biotechnol.* **2013**, *31*, 553.
- [48] C. Liu, A. F. Faria, J. Ma, M. Elimelech, *Environ. Sci. Technol.* **2017**, *51*, 182.
- [49] N. Encinas, C.-Y. Yang, F. Geyer, A. Kaltbeitzel, P. Baumli, J. Reinholz, V. Mailänder, H.-J. Butt, D. Vollmer, *ACS Appl. Mater. Interfaces* **2020**, *12*, 21192.
- [50] G. Y. Liu, V. Nizet, *Trends Microbiol.* **2009**, *17*, 406.
- [51] J. R. Kamitakahara, W. J. Polglase, *Biochem. J.* **1970**, *120*, 771.